Green Chemistry

PAPER

View Article Online
View Journal | View Issue

Cite this: *Green Chem.*, 2024, **26**, 542

Hydrophobic and water resistant fish leather: a fully sustainable combination of discarded biomass and by-products of the food industry†

Marta Fadda, *[a,b] Arkadiusz Zych, [a] Riccardo Carzino,[c] Athanassia Athanassiou [a] and Giovanni Perotto *[a]

The food industry produces a large amount of food byproducts that, when appropriately valorized, can become a renewable source of sustainable materials. The valorization of these byproducts requires a new set of green technologies. For example, fish farming, one of the fastest growing sectors, uses only 30% to 40% of the fish as food, with the remaining 60% to 70% being a byproduct. One example of valorization of fish byproducts is the upcycling of fish skin into leather. This new fish leather has interesting properties, in part due to its microstructure, but also has new shortcomings like the high hydrophilicity and water absorption. To mitigate these issues, a water protecting coating was developed using only two other food byproducts: epoxidized soybean oil and the fatty acid trimer Pripol. These two building blocks were deposited on leather and then crosslinked to create a strong network that made leather hydrophobic, with a water contact angle >120° without the need for fluorine or silicone chemistry or the use of nanoparticles. The coating was applied *via* dip-coating and was cured at low temperature as required by fish leather without the need for initiators, catalysts, which are mostly toxic, or UV light. The same strategy could also be applied to cotton, showing that its application is not limited only to leather. The coating showed good adhesion to the substrate and excellent water resistance, making the leather and the cotton hydrophobic and substantially reducing the water absorption, without changing the breathability, flexibility and microstructure of the substrate. This work demonstrates how high performing materials can be created within a green chemistry and circular economy framework, with results that can be relevant for other textile materials, contributing to the effort for developing sustainable alternatives for providing hydrophobicity.

Received 23rd October 2023,
Accepted 23rd November 2023

DOI: 10.1039/d3gc04048h

rsc.li/greenchem

1. Introduction

Nowadays, the fastest growing food production sector is marine aquaculture,[1] where the Atlantic salmon (*Salmo salar*) represents 90% of the production.[2] This fast growth and the related disposal of increasing quantities of waste generated upon fish processing are causing serious damage to the environment and to the ecosystem.[3] In particular, the skin of salmon is one of the main wastes of the aquaculture industry that often remains unused: transforming the unused fish skin into leather could enable it to become an industry-shifting material, in particular in fashion.[4] Leather from fish skin is more breathable, thinner and stronger than lamb and cow leather, due to the intertwining of its fibers with respect to the parallel distribution of the fibers in more traditional leathers; today it represents less than 1% of the global leather sales. Being a new material, fish leather has a new set of challenges, some of which are the result of its peculiar structure. Fish skin and consequently fish leather (FL) are comprised of an interweaving of protein fibers, with collagen being the main component. As previously reported, collagen with its triple helical structure made of three polypeptide chains is the main component of the extracellular matrix.[5] Fibrillar collagen, collagen type I, is the most common and is organized in fibrils and fibers, giving support to many parts of the body (*e.g.* skin, bones, cartilage, tendons).[5] Since FL is made of collagen, the presence of several hydrophilic groups (*e.g.* amino, carboxyl and hydroxyl groups) makes it a hydrophilic material very sensitive to water once tanned into leather.[6] In addition, the fibrillary microstructure creates high porosity and surface area, contributing to the enhancement of its wettability properties.[7]

[a]*Smart Materials, Istituto Italiano di Tecnologia (IIT), Via Morego 30, 16163 Genoa, Italy. E-mail: m.fadda@inrim.it, giovanni.perotto@iit.it*
[b]*Dipartimento di Informatica, Bioingegneria, Robotica e Ingegneria dei Sistemi (DIBRIS), University of Genoa, Via all'Opera Pia 13, 16145 Genoa, Italy*
[c]*Materials Characterization Facility, Istituto Italiano di Tecnologia (IIT), Via Morego 30, 16163 Genoa, Italy*

† Electronic supplementary information (ESI) available. See DOI: https://doi.org/10.1039/d3gc04048h

Since the leather and fashion industries are aiming to become more sustainable sectors by reducing their environmental impact and their use of toxic chemicals,[8] a new waterproofing treatment for fish leather should avoid the use of fluorine or silicone chemistry. In previous years, several solutions have been proposed in terms of hydrophobic coatings or treatments for leather even if not specifically for fish leather. For instance, Serenko *et al.* proposed fluorine silane as a hydrophobic agent in ethanol to spray on leather;[7] Qiang *et al.* prepared a polyether organosilicone succinate ester mixed with sulfated neatsfoot oil and oxidized-sulfited fish oil to make a new leather fatliquor to improve the waterproofing ability of the leather;[9] Feng *et al.* developed a polymerized vinyltriethoxysilane coating deposited on the leather by using a low-pressure and cold plasma technique increasing the hydrophobicity of the leather itself;[10] Ma *et al.* sprayed two layers on leather, one made with polyacrylate emulsion and the other made with ethanol dispersion of hydrophobic silica nanoparticles.[6] However, in the last few years the environmental impact of materials and processes is becoming more and more relevant, also in the production of hydrophobic coatings for textiles. Therefore, researchers and industries are looking for materials that are greener, more eco-friendly, bio-based, and easier to recycle or manage once discarded. Therefore, now the market is demanding not only fluorine-free but also nanoparticle-free solutions: indeed, the $-CF_3$ harmfulness for the environment and for human beings has been stated, as well as the fact that inorganic nanoparticles are not degradable, representing a problem not only for the environment itself, but also in terms of recycling and complexity of waste management.[11] For this reason, in this work the development of a fluorine-free, nanoparticle-free and fully sustainable coating to make the FL hydrophobic has been the main effort.

In this work, FL was obtained by partially tanning with mimosa extract, in order to increase the bio-based content in the final material (Fig. 1).

For waterproofing the leather, we aimed at developing a new material that can be used as a coating using only building blocks that were obtained from the valorization of food byproducts. Because of this, epoxidized soybean oil and fatty acid derived Pripol were used as ingredients. Few previous works used epoxidized oils and resins to improve the waterproofing ability of leather. For instance, epoxidized vegetable oils have been used during the tanning together with a catalyst in order to obtain a crosslinked system that comprises the collagen of the leather and the oil, resulting in a flexible and water-resistant chamois leather (CN101550459B) or salmon leather (CN101240355A). Soybean oil has been considered because it is produced in excess in many geographical areas with respect to its demand for consumption in cooking.[12] Furthermore, as triglyceride, it has unsaturated sites that could be used to introduce functional and highly chemically reactive groups such as epoxides, making the epoxidized soybean oil (ESO).[13] Last but not least, ESO has been already used to make water-resistant materials and coatings for natural films and cellulose-based fabrics. For instance, Ge *et al.* coated starch-based films with an acrylated epoxidized soybean oil-based coating that was crosslinked and polymerized using UV light, obtaining a smooth layer on the top of the starch films, imparting hydrophobicity and limiting their water absorption.[14] Miao *et al.* fabricated epoxidized soybean oil-based paper composites, polymerizing the oil directly on the surface and within the interspaces of the paper cellulose fibers in order to improve the water resistance of paper.[15] In addition, we propose to use ESO together with a second bio-based building block: Pripol, a complex mixture of polycarboxylic acids (mostly trimers and some dimers of fatty acids), that is produced by coupling reactions of bio-based unsaturated and partially hydrogenated fatty acids (mainly oleic and linoleic).[16] The carboxylic groups of Pripol can react with the epoxide groups of ESO crosslinking the two liquids and forming a stable network.[17] Previously, a dimer acid was considered to perform the open-ring reaction of bisphenol-A epoxy resin to synthesize a UV-curable epoxy acrylate oligomer by Liang *et al.*;[18] Li *et al.* prepared a vitrimer elastomer by crosslinking a commercial glycidylamine epoxy with a vegetable oil-derived dimer acid using a two-step curing process.[19] Since the collagen of leather has several carboxyl groups, this reaction could occur with the substrate, contributing to good adhesion. Finally, since Pripol and ESO are fatty acids and thanks to their long chains, they are expected to provide a good solution to improve the water resistance of leather.

The crosslinking of the ESO/Pripol coating on FL was evaluated spectroscopically and *via* quantification of the gel fraction. Water protection was characterized by measuring the water contact angle and by monitoring its change over time, to

Fig. 1 Photo of salmon fish leather obtained by mimosa and chromium tanning.

demonstrate the durability of waterproofing. On the other hand, the breathability and flexibility of the FL before and after coating were characterized to demonstrate the preservation of these properties. For the first time, three materials, obtained by valorization of biomass and by-products of the food industry, were combined to show how a green and circular approach could be used to obtain high performing materials.

Last but not least, we showed how these results can translate to more common textile fabrics like cotton, conferring hydrophobicity and demonstrating the versatility of this green approach.

2. Materials and methods

2.1. Materials

Epoxidized soybean oil (ESO) (M_w = 950 g mol^{-1}; 4 epoxides per molecule) was purchased from ATP R&D srl. PRIPOL™ 1040-LQ-(GD) (Pripol) (M_w = 830 g mol^{-1}; 2.78 carboxylic acid groups per molecule) was purchased from Croda. Ethyl acetate was purchased from Sigma Aldrich. Salmon skin leather tanned with mimosa extracts was kindly provided by ViaTalenta Foundation (Switzerland). Deionized water was obtained from Milli-Q Advantage A10 purification system. All chemicals were analytical grade and used as received.

2.2. Preparation of the solution

55.7 g of Pripol was mixed with 44.3 g of ESO until complete homogenization. The final mixture, labeled as PESO, was dissolved in ethyl acetate at different concentrations: 1, 5, 10 and 15% (w/w). The solutions were labeled as 1% PESO, 5% PESO, 10% PESO, and 15% PESO, respectively. A summary of the procedure is shown in Fig. 2A.

2.3. Preparation of coated leather and coated cotton

Fish leather or cotton fabric was cut into pieces (2 cm × 3 cm) and dip coated in the solutions. The samples were dried at room temperature in a fume hood for 3 hours until the complete evaporation of the solvent. Afterwards, they were placed in an oven at 80 °C for 2 weeks for curing. The samples were labeled as PESO 1, PESO 5, PESO 10, and PESO 15 for coated FL and PESO 15-CF for coated cotton fabrics. A summary of the fabrication steps is shown in Fig. 2B. In addition, free standing films (film) of the coating material were made by casting 20 mL of 15% PESO solution in a round shaped Teflon dish with a diameter of 8 cm. The solvent was allowed to evaporate under a fume hood and the resulting material was cured in the oven to give a freestanding material.

2.4. Evaluation of the crosslinking

The crosslinking of the PESO coating was evaluated on 5 cm × 1 cm samples of PESO 1, PESO 5, PESO 10, and PESO 15, and untreated FL was used as control, as well as 1 cm × 1 cm pieces of the film. The samples were weighed before and after the application of the coating to calculate the weight of the coating. The crosslinking after curing was evaluated in terms of gel fraction (GF), representing the amount of sample that was crosslinked and thus, was not soluble anymore: after curing, the samples were conditioned at 0% R.H. by using anhydrous silica gel for 48 hours, and weighed (W_i). Afterwards, the samples were placed in 10 mL of ethyl acetate for 24 hours, left to dry under a hood for 24 hours, conditioned in 0% R.H. by using anhydrous silica gel and weighed to obtain W_f. By using eqn (1) GF was obtained:

$$\mathrm{GF}(\%) = \frac{W_f}{W_i} \times 100 \quad (1)$$

2.5. Chemical characterization: ATR-FTIR and XPS

Chemical characterization of Pripol, ESO, PESO, film, PESO 1, PESO 5, PESO 10, PESO 15, and untreated FL was made by using a single-reflection ATR accessory with a diamond crystal (MIRacle ATR, Pike Technologies) coupled to an FTIR spectrophotometer (VERTEX 70v FTIR, Bruker). The spectral region scanned was 4000–600 cm^{-1} with a resolution of 4 cm^{-1}. The spectra were normalized to their maximum.

Elemental analysis of PESO 15 and untreated FL's surface were investigated by using X-ray photoelectron spectroscopy (XPS). An electron spectrometer (Lab2, Specs, Berlin, Germany) equipped with a monochromatic X-ray source (set at 1486 eV) and a hemispherical energy analyzer (Phoibos, HSA3500, Specs, Berlin, Germany) was used. The voltage of the Al Kα X-ray source and the current were set at 13 kV and 8 mA, respectively. The pressure in the analysis chamber was ~1 × 10^{-9} mbar.

2.6. Water contact angle

Dynamic water contact angles were measured for untreated FL, PESO 1, PESO 5, PESO 10, PESO 15, film, uncoated cotton fabric and PESO 15-CF using a contact angle goniometer (OCA-20 DataPhysics, Instruments GmbH, Filderstadt, Germany) at room temperature. Deionized water droplets of 10 μL were deposited on the surface and the contact angle was calculated from the side view with the help of the built-in software at specific time points (0, 5, 10, 15, 20, 25, 30, 35 and 40 minutes). Six measurements for each coating were taken to ensure repeatability. A sheet of polytetrafluoroethylene (PTFE) was used as a control to exemplify a hydrophobic and non-absorbent material.

2.7. Water contact angle after water immersion

The evaluation of the preservation of the hydrophobicity of the coatings after washing with water was done on PESO 15 samples. They were placed in 10 mL of deionized water for 24 hours. Afterwards, they were taken out, and left to dry under the hood for 24 hours. The contact angle was measured by using a contact angle goniometer (OCA-20 DataPhysics, Instruments GmbH, Filderstadt, Germany) at room temperature, following the same steps described above (section 2.6).

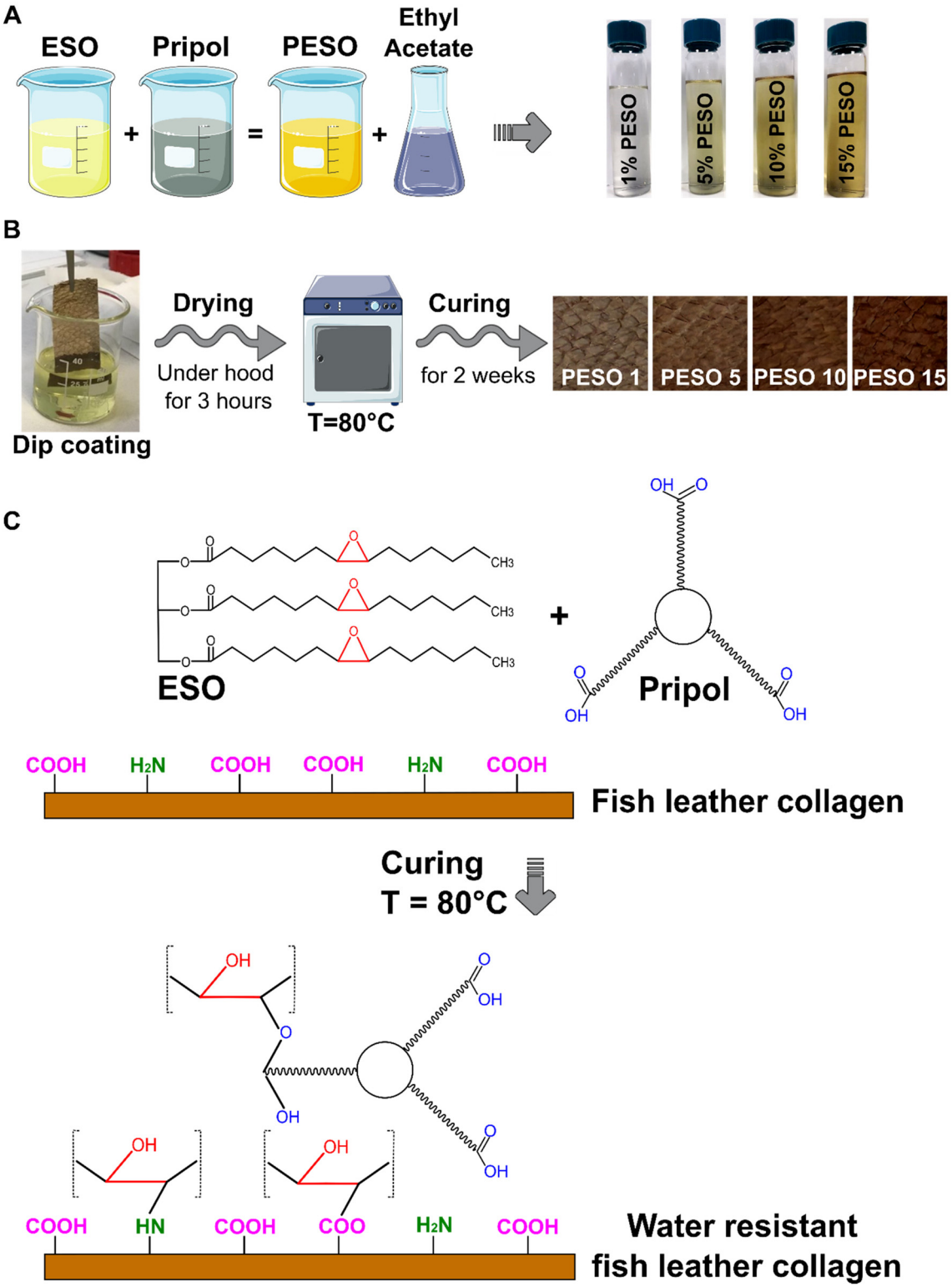

Fig. 2 (A) Schematic illustration of solution fabrication steps. (B) Schematic illustration of coating fabrication steps: dip-coating, drying and curing in an oven at 80 °C for two weeks. The photos show PESO 1, PESO 5, PESO 10 and PESO 15 coatings on FL. (C) Schematic illustration of the preparation of the coatings with the materials involved (ESO, Pripol and FL) with all the involved functional groups and chemical linkages between them after curing in evidence.

2.8. Water uptake and water vapor permeability

For the water uptake evaluation, PESO 1, PESO 5, PESO 10, PESO 15, untreated FL and film specimens (1 cm × 1 cm) were conditioned at 0% R.H. by using anhydrous silica gel and weighed by using a sensitive electronic balance ($W_{0\%}$). Afterwards, they were placed in a sealed chamber under different relative humidity conditions (% R.H.), 11, 44, 84 and 100, obtained by using LiCl, K_2CO_3 and KCl saturated saline solutions and water, respectively. The samples were weighed after 1 day in the chamber ($W_{RH\%}$). The water uptake (WU) was evaluated by using eqn (2):

$$\mathrm{WU}(\%) = \frac{W_{RH\%} - W_{0\%}}{W_{0\%}} \times 100 \quad (2)$$

where $W_{RH\%}$ is the weight of the samples under different R.H. conditions and $W_{0\%}$ is the weight of the samples at 0% R.H. Five samples were tested to ensure the reliability of the measurement.

The water vapor permeability (WVP) of untreated FL, PESO 1, PESO 5, PESO 10, PESO 15, uncoated cotton fabrics and PESO 15-CF, was evaluated under 100% relative humidity gradient ΔRH (%) by following the ASTM E96 standard method. 400 μL of deionized water were placed in the permeation chambers of 7 mm inner diameter and 10 mm height to accomplish ΔRH. Samples were mounted on the top of the permeation chamber, sealed and placed at 0% R.H. by using anhydrous silica gel. The chambers were weighed every hour for 7 consecutive hours by using a sensitive electronic balance (0.0001 g accuracy) to monitor the transfer of water from the chamber, through the sample, to the desiccant, evaluating the water mass loss. The water mass loss was plotted as a function of time. The slope of each line was calculated by linear regression. Afterwards, the water vapor transmission rate (WVTR) was determined by using eqn (3):

$$\mathrm{WVTR}\,(\mathrm{g}\,(\mathrm{m^2 d})^{-1}) = \frac{\mathrm{slope}}{A} \quad (3)$$

where A is the area of the sample.

The water vapor permeability (WVP) of the samples was calculated by using eqn (4):

$$\mathrm{WVP}\,(\mathrm{g}\,(\mathrm{md\,Pa})^{-1}) = \frac{\mathrm{WVTR} \times L \times 100}{p_s \times \Delta\mathrm{RH}} \quad (4)$$

where L is the thickness of the sample (m), p_s is the saturation water vapor pressure at 25 °C (Pa). Every measurement was replicated three times to ensure the reliability of the results.

2.9. Morphological analysis

The microstructure of the surface and cross-section of the treated and untreated FL, treated and untreated cotton fabric was investigated by using a Scanning Electron Microscope (SEM; JSM-6490LA, JEOL, Japan) with 10 kV acceleration voltage. The samples were previously mounted on a tilted stub, framed with silver paste, and sputter-coated (Cressington Sputter Coater – 208 HR) with a 10 nm thick layer of gold.

2.10. Mechanical characterization

PESO 1, PESO 5, PESO 10, PESO 15 and untreated FL were tested with uniaxial tension tests on a dual column universal testing machine (Instron 3365). The samples were cut in dog bone shape (ten samples were tested for statistical analysis) with a width of 4 mm and length of 25 mm. They were conditioned at 24 °C and 50% R.H. in a humidity chamber (Espec SH-262 Environmental Chamber). Displacement was applied at a rate of 5 mm $\mathrm{min^{-1}}$. The Young's modulus and the elongation at break were calculated from the stress–strain curves.

2.11. Thermal characterization

Thermogravimetric analysis (TGA) of PESO 15 and untreated FL was performed by using a TGA Q500 (TA Instruments, USA) instrument. Measurements were performed by placing the samples (7 mg) in platinum pans under an inert N_2 flow (50 mL $\mathrm{min^{-1}}$) in the temperature range from 30 to 800 °C with a heating rate of 10 °C $\mathrm{min^{-1}}$.

3. Results and discussion

3.1. Evaluation of crosslinking

The PESO films and the coated fish leather sample were prepared according to the schematic shown in Fig. 2. Table 1 reports the weights of the coatings of PESO 1, PESO 5, PESO 10 and PESO 15 on FL and their gel fraction (GF). The coating represents 2, 8, 11, and 22% of the mass of the final material for PESO 1, PESO 5, PESO 10, and PESO 15, respectively. The efficacy of the curing step, evaluated in terms of GF, showed that for all samples it was very high, being always >97%, demonstrating that the temperature and time used for the crosslinking were optimal. The GF of the film was high (>92%) demonstrating the successful crosslinking between Pripol and ESO. The conjugation between PESO and collagen, which was expected to happen due to the presence of a large number of –COOH and $–NH_2$ functions on the surface of the collagen, could not be evaluated quantitatively.

For the purpose of this paper only building blocks from the valorization of food byproducts were used, and all results refer to that, in order to reduce the curing time we studied the possibility of adding a catalyst. Two catalysts were tested: *N*,*N*-1,1,3,3-tetramethylguanidine and 1-ethylimidazole. As shown in Fig. S1,† with these catalysts a gel fraction higher than 95% could be achieved by curing PESO at 80 °C for 48 hours, significantly reducing the curing time.

Table 1 Weight (mg) and GF (%) of PESO 1, PESO 5, PESO 10, PESO 15 and film

Sample	Weight ± s.d. (mg)	GF ± s.d. (%)
PESO 1	4.7 ± 0.7	98.1 ± 1.0
PESO 5	19.2 ± 3.0	98.9 ± 0.1
PESO 10	30.1 ± 1.7	97.8 ± 0.2
PESO 15	53.2 ± 2.4	97.3 ± 0.5
Film	220.2 ± 9.1	92.3 ± 1.1

3.2. Chemical characterization: ATR-FTIR and XPS

To study the crosslinking reaction between the Pripol and ESO, from the chemical point of view, we used FTIR on the raw materials, the blend of the two components and a freestanding film of the cured material (Fig. 3A). As can be noticed, both Pripol and ESO presented the peaks at 2925 and 2855 cm^{-1} assigned to the asymmetric and symmetric stretching of CH_2, respectively. These peaks were still visible in PESO and cured free standing film samples. The peak assigned to the stretching of C=O was observable at 1707 cm^{-1} and at 1741 cm^{-1} for Pripol and ESO, respectively, with the difference in the peak position due to the fact that Pripol has free carboxylic acid whereas ESO has three ester groups. Comparing this spectral region before and after curing, it can be noticed how before the curing the intensity of the free carboxyl was higher,

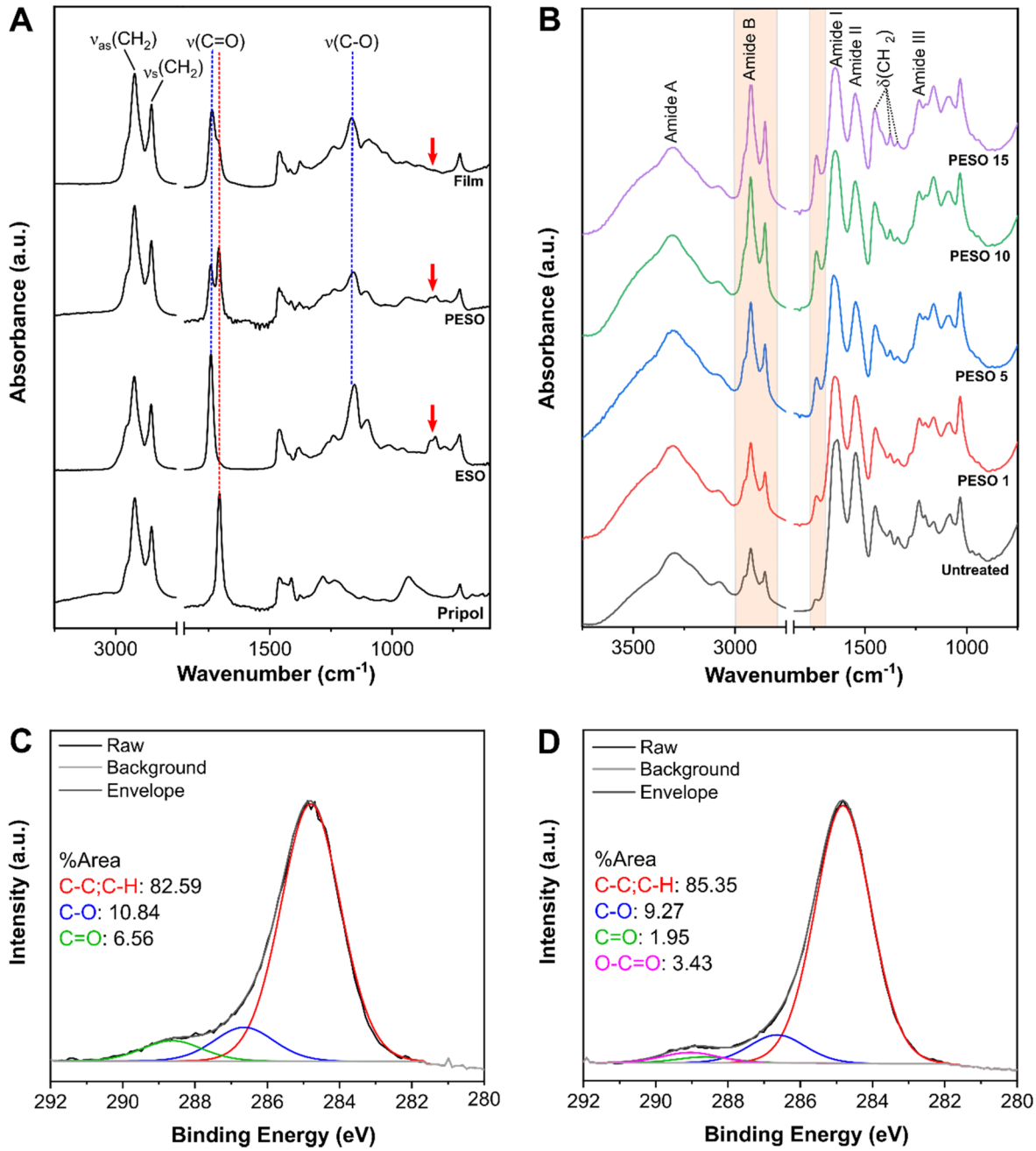

Fig. 3 (A) ATR-FTIR spectra (from the bottom) of Pripol, ESO, PESO, and film with the characteristic peaks of ESO (blue dotted line) and Pripol (red dotted line). Red arrows highlight the peaks relative to the epoxy groups of ESO. (B) ATR-FTIR spectra (from the bottom) of untreated FL, PESO 1, PESO 5, PESO 10 and PESO 15 with all the characteristic peaks of collagen Type I. The reddish bands highlight the peaks at 2925, 2855 and 1741 cm^{-1}. (C and D) XPS spectra of C 1s for untreated FL and PESO 15, respectively.

because of the higher molarity of free –COOH. After curing, the ester vibration became predominant, because of the reaction between the carboxyl groups of Pripol with the epoxy groups of ESO, confirming the formation of the crosslinked network between Pripol and ESO after the curing step. The peak at 1155 cm^{-1} was assigned to the stretching of C–O and it was clearly visible in ESO, PESO, and free standing film spectra, but not in the spectrum of Pripol. Therefore, it was evident that these groups were part of the molecule of ESO and they did not take part in the reaction. Finally, in the ESO spectrum the peak at 823 cm^{-1} relative to the epoxy groups, highlighted by the red arrows in Fig. 3A, was visible before curing but not after, as a further demonstration of the crosslinking reaction of the epoxy groups with the carboxyl groups of Pripol. All the assignments were done based on ref. 20–22.

To study the substrate and its functional groups involved in the reaction with the coating material, the FTIR spectra of untreated and coated FL were acquired and reported in Fig. 3B. In particular, it shows, from the bottom to the top, the FTIR spectra of the untreated FL, PESO 1, PESO 5, PESO 10 and PESO 15 samples. All these samples showed the characteristic peaks and structure of collagen Type I: the peaks at 3300 and 3080 cm^{-1} were assigned to the stretching of N–H and O–H, respectively, relative to amide A; the peaks at 2925 and 2855 cm^{-1} were assigned to the asymmetric and symmetric stretching of CH_2, respectively, relative to amide B; the peaks at 1645 and 1545 cm^{-1} were assigned to the stretching of CH (amide I), and to the vibrations on the plane of the N–H bond and to the stretching of C–N, respectively (amide II); the peaks at 1450, 1375 and 1337 cm^{-1} were assigned to the asymmetric bending of CH_2, CH_3 and CH_2, respectively, corresponding to the stereochemistry of the pyrrolidine rings of proline and hydroxyproline; the peak at 1234 cm^{-1} was assigned to the stretching of C–N, relative to amide III. All the assignments were done based on these references.[23–25] These spectra revealed a strong contribution of the substrate, since the chemical structure of the collagen was still clearly visible after the application of the coating. An increase in the intensity of the peaks at 2925 and 2855 cm^{-1} relative to the CH_2 vibration was observed between the untreated and the coated FL, especially in the FL with most of the coating on it, PESO 15. These peaks belong to the long CH_2 chains in the fatty acids comprising the free standing film sample. As expected, the higher the amount of the coating on FL, the higher their intensities. The same behavior can be observed for the peak at 1741 cm^{-1}, assigned to the stretching of C=O, visible both in the untreated and coated FL, with an increase in its intensity with the increase in the amount of the coating on FL.

To further characterize the change in surface chemistry due to the coating, XPS was used, comparing the untreated and PESO 15 coated FL. The XPS spectrum relative to the C 1s for the untreated and coated FL are reported in Fig. 3C and D. From the analysis of the peak relative to C 1s of the untreated FL three peaks were found and based on their binding energy were assigned to C=O (green), C–O (blue) and C–C (red). These groups represented the functional groups that were expected to be found in collagen type I comprising the FL. The coated sample showed an additional group, O–C=O (in magenta in the graph) and a slight increase in the intensity of C–C and C–H peaks. Both changes were signatures of the presence of the coating, which is rich in O–C=O, C–C and C–H due to Pripol and ESO.

3.3. Morphological analysis

As the initial step, the FL sample was distinguished in front and back parts, where the front was relative to the scaly pattern typical of the fish skin. For this kind of analysis, the expected fibrous structure of FL was investigated by SEM (see ESI, Fig. S2†). In Fig. S2A and B† top-view images relative to the front are reported. As can be noticed, the surface is covered in fibers that are not distributed homogeneously and in a disorganized manner, characterized by random interweaving and entanglement. On the other hand, the investigation of the back part of the sample (Fig. S2C and D†) showed a more organized structure of the fibers. As shown in Fig. 4A–C and more images in Fig. S2E and F,† in the back of the leather and in the cross section, collagen fibers comprising the leather were in a well-organized structure, with bundles of fibers with a preferential orientation and stacked at an angle of about 90° between layers. Similar results were observed by Wairimu *et al.* on the skin of a different type of fish, the Nile perch fish.[26] The higher magnifications image, Fig. 4C, of our salmon leather, showed that the single fibers were organized into smaller fibrils. This is the typical structure of collagen,[27] the main component of leather that was cross-linked together in the tanning process. To understand how the microstructure of the coated FL appeared and if the coating brought some modifications in it, SEM images of the top view and cross-section of PESO 15-coated FL were acquired with the same magnifications, as comparisons (Fig. 4D–F). The coated samples showed no visible changes in the microstructure, confirming a very thin layer of PESO deposited onto the fibrous leather. Unfortunately, from these images no information about the thickness of the coating can be obtained. However, as can be noticed in Fig. 7D, the SEM image of the cross-section of PESO 15-coated cotton revealed a thin layer (with a thickness that can be estimated in the 100 nm range) around the cotton fiber, as highlighted by the red arrow. It can be deduced that the thickness of the coating around fish leather fibers was characterized by similar values. To visualize the coating and its interaction with the substrate, a more concentrated coating was prepared using a 50 wt% PESO solution in ethyl acetate. This far more concentrated coating applied on leather changed significantly some macro-properties of the substrate, making it darker in color, decreasing its softness and increasing its stiffness. The morphology of this thick coated samples, as reported in Fig. S3† showed that the multi-layer structure of the collagen fibers was embedded in the oil-based coating (Fig. S3A†), explaining the macroscopic change of properties. Moreover, higher magnifications of the collagen layers,

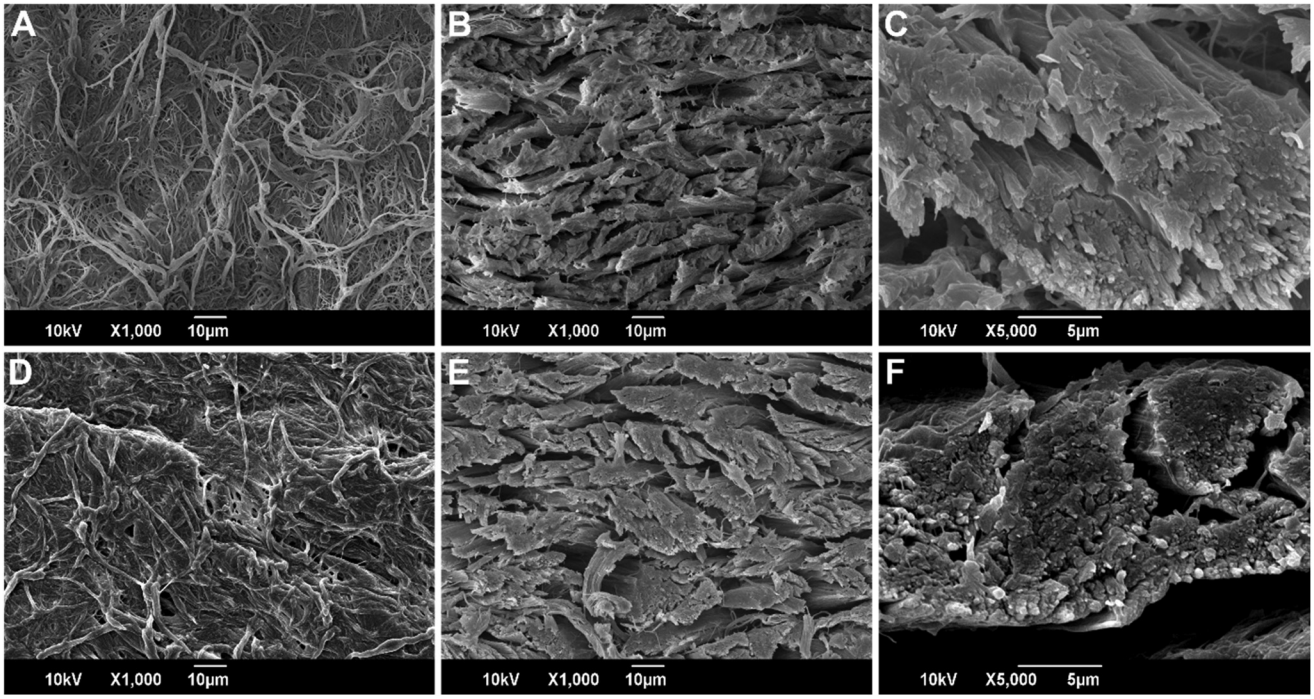

Fig. 4 (A–C) SEM image of the top view and cross-section of the untreated FL. (D–F) SEM image of the top view and cross-section of PESO 15.

revealed how the coating was deposited between each fiber but not in between the smaller fibrils (Fig. S3B†) and its thickness could be estimated in the ~10 μm range.

3.4. Water contact angle

Fig. 5A reports the water contact angle (WCA) of untreated FL, PESO 1, PESO 5, PESO 10, PESO 15, film and PTFE after 60 seconds. As can be noticed, while untreated FL presented a hydrophilic behavior with a WCA of ~80°, each of the coated FL showed a strong hydrophobic behavior, with a WCA of ~130°. Comparatively, PTFE had a WCA of ~110°. The WCAs were comparable and outperforming with respect to previous results obtained for oil-based bio-coatings reported in the state of the art. For instance, Zhang *et al.* reported a WCA of ~100° for the proposed UV-curable polyurethane and castor oil-based coating;[28] Parvathy *et al.* developed a coating derived from castor oil based epoxy methyl ricinoleate for paper obtaining a WCA of up to 97°;[29] and Vijayan *et al.* joined a bio-acrylate linseed oil-based resin with beeswax to develop a coating for paper in order to improve its barrier properties and to impart hydrophobic properties, obtaining WCAs of up to 90°.[30] This high WCA of the coated FL, compared to the two reference samples, can be ascribed to the fibrillary microstructure of the substrate, and confirmed that the deposited coating was very thin and did not change the morphology of the substrate but was rather conformal to it. To confirm this statement the Cassie–Baxter model was applied on this system (eqn (5)):

$$\cos\theta = \sigma_c \cos\theta_c + \sigma_a \cos\theta_a \quad (5)$$

where $\sigma_a = 1 - \sigma_c$ and $\theta_a = 180°$, therefore the eqn (5) becomes (eqn (6)):

$$\cos\theta = \sigma_c(\cos\theta_c + 1) - 1 \quad (6)$$

As previously reported by Bormashenko *et al.*[31] The fraction of the coating–liquid interface (σ_c) can be considered 1 for the freestanding film sample, since its surface is flat and therefore without air pocket. Using eqn (6), the fraction of the interface was calculated for all coated fish leather, where θ is the WCA measured on the sample after 60 seconds, while θ_c is the WCA of the freestanding coating film after 60 seconds. Substituting all these terms in eqn (6), σ_c for all the coated fish leather samples was found to be 0.47, showing how the fibrillary microstructure of the substrate reduced the contact area with the water droplet.

At the end of this initial study, all the coatings, whatever the amount of the oils on them, were considered equally functional. However, an initial change in color was noticed with PESO 15, making the substrate slightly darker. As can be expected, the color is one of the most appreciable properties due to the final application in fashion, therefore it was decided to set this as the higher concentration that could be tested.

To characterize the durability of the improved hydrophobicity, WCA was studied for up to 40 min (Fig. 5B). Untreated FL initially showed a hydrophilic behavior with a WCA of 80°, and after only one minute there was complete absorption of water. On the other hand, PESO 15 showed a hydrophobic behavior that lasted up to 40 minutes with a final WCA of ~100°. The WCA of the film was ~100° after 60 seconds and decreased to ~80° after 40 minutes, similar to the decreasing trend shown by the PESO coated samples. The reason for the reduction of

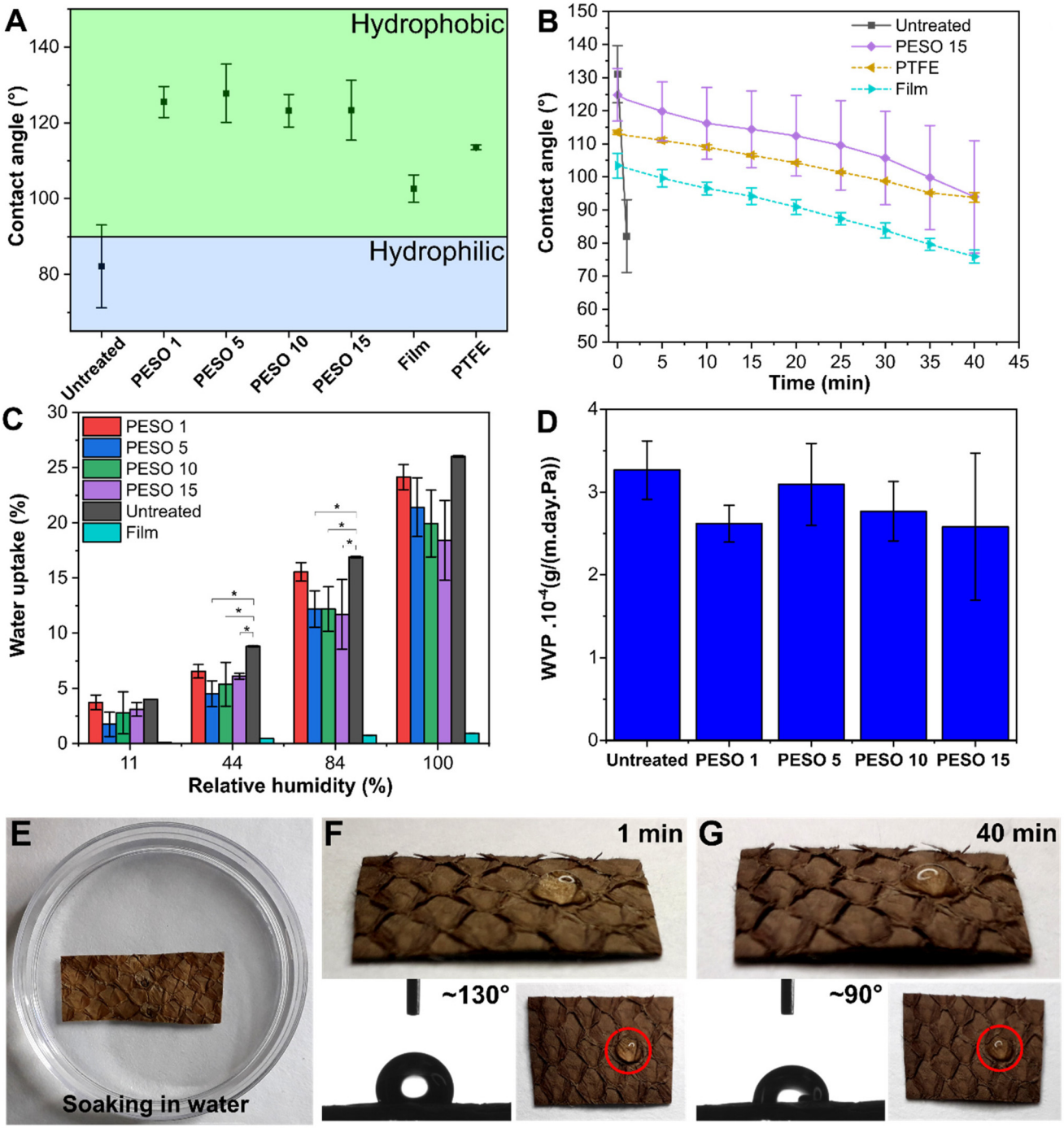

Fig. 5 (A) WCA (°) of untreated FL, PESO 1, PESO 5, PESO 10, and PESO 15, film and PTFE after 60 s. (B) WCA (°) *vs.* time (min) of untreated FL, PESO 15, film and PTFE. (C) Water uptake (%) of untreated FL, PESO 1, PESO 5, PESO 10, PESO 15, and film at different %R.H. * ANOVA test for $p < 0.05$. (D) WVP (g m^{-1} day^{-1} Pa^{-1}) of untreated FL, PESO 1, PESO 5, PESO 10, and PESO 15. (E–G) Evaluation of the stability of the coating after washing: (E) soaking of PESO 15 in water, WCA (°) with pictures of the drop at (F) 1 and (G) 40 min.

the WCA with time was examined by comparing the wetting behavior of the film sample and PESO 15 with PTFE, a well-known non-water-absorbing surface. As can be noticed, the behavior of the WCA of PESO 15 and film is very similar to that of PTFE, so we can safely assume that the WCA reduction of PESO 15 is mainly due to the evaporation of water and is not related to the absorption of water by the FL. In addition, the comparison between the droplet's volume and base diameter on PESO 15 and film with those of PTFE (see Fig. S4A†) has confirmed much more the previous statement, also because a similar behavior for PTFE has been already reported in the literature.[32]

Furthermore, the volume of the droplet absorbed by PESO 1, PESO 5, PESO 10 and PESO 15 during the WCA experiment was calculated and reported in Fig. S4B.† As can be noted,

PESO 1 started to absorb water immediately, whereas PESO 5 and PESO 10 protected the FL from the absorption of water up to 15 minutes. However, PESO 15 was demonstrated to be water resistant up to 40 minutes, as also demonstrated by the pictures of the drops at 0, 20 and 40 min.

Using this method to analyze the results for PESO 1, PESO 5, and PESO 10, (Fig. S4C and S4D†), we can conclude that PESO 1 deposited only a small quantity of coating and did not provide a sufficient water resistant effect to the leather, while PESO 5 and PESO 10 maintained their hydrophobicity until 20 and 30 minutes respectively, but they both started to absorb water after 15 minutes (Fig. S4B†).

This is an interesting result and shows how the combination of the microstructure and hydrophobicity can be exploited to create a material that is produced entirely from the valorization of byproducts, with advanced functional properties that are comparable to PTFE.

3.5. Water uptake and water vapor permeability

To test if, together with improved hydrophobicity, the coating could offer protection to FL from moisture absorption, samples were conditioned at different relative humidities (% R.H.). Fig. 5C reports the water uptake of untreated FL and PESO 1, PESO 5, PESO 10, PESO 15, and film sample. As can be observed, the film sample did not show an increase in mass, due to its hydrophobic and oil-based nature. Coated and untreated FL increased in mass when exposed to high relative humidity, due to moisture absorption, but the coated samples showed reduced water absorption. For instance, the ANOVA test ($p < 0.05$) revealed that at 44 and 84% R.H., two realistic humidity conditions, PESO 5, PESO 10 and PESO 15 protected the substrate from moisture, reducing the absorption of water from 17% to 12% at 84% R.H.

As mentioned, one of the appealing features of FL is its higher breathability, when compared to cow leather. To ensure that the coating did not hamper this property, WVP of untreated FL, PESO 1, PESO 5, PESO 10, and PESO 15 was measured and the results are reported in Fig. 5D. As can be noticed, none of the coatings affected the WVP, and consequently, the breathability of the FL. This result was due to the thin and conformable coating that could be deposited in order not to change the porosity and the microstructure of the substrate, as discussed before and examined also in section 3.3.

3.6. Preservation of the hydrophobicity after washing and solvent resistance

One of the requirements for the successful application of FL, is the perseverance of the coating's functionality after the immersion of the samples in water to simulate cleaning or resistance to weather factors such as rain. To study this, PESO 15 samples were fully submerged in 10 mL of MilliQ water (see Fig. 5E), after which they were dried at ambient temperature and humidity for 24 hours. The WCA measured after this step, reported in Fig. 5F (time, 60 seconds) and 5G (time, 40 minutes) showed that the contact angle after 60 seconds was ~130°, while at 40 minutes it was ~90°, confirming the preservation of the hydrophobicity induced by the coating. The reason for the reduction of the WCA with time was due to the evaporation of water without absorption from the substrate, as discussed above. Furthermore, as highlighted by the red circles around the drops in the pictures, no wicking of water droplets was observed, confirming the evaporation of water and the excellent waterproofing of the coated leather. This result verifies the protective effect of the coating on the FL: even after immersion for 24 hours in water, the coating was still adhering to the substrate and it was able to protect it from water droplets. If the coated FL got wet after a heavy rain, the coating would continue to protect the leather once dried again.

The solvent resistance of the coating material (film) against common solvents such as ethanol, acetone, ethyl acetate and water was evaluated in terms of gel fraction. As reported in Table S1 (see the ESI†), the coating showed gel fraction values greater than 95% for all the solvents tested. This achieved result demonstrated that the coating could preserve its crosslinking strength also in the case of successive organic solvents-based treatments on FL (*e.g.* dying, finishing) without losing its functionality, even if, today, most of them are water-based.

3.7. Mechanical characterization

Fig. 6A shows the stress–strain curves of untreated FL, and FL coated with PESO 1, PESO 5, PESO 10, and PESO 15. The untreated FL presented the typical trend of collagen fibers[33] with three regions (dotted lines in the graph): toe, heel and linear. As reported by Gutsmann *et al.*, the toe region is due to the removal of macroscopic crimps in the collagen fibrils, the heel region is caused by the reduction of the disorder in the lateral molecular packing, and the linear region is due to the stretching of collagen triple helices or of the crosslinks between helices.[33] As can be noticed, PESO 1 presented the same trend as the untreated FL, therefore, the coating did not influence the mechanical properties of the substrate. On the other hand, PESO 5, PESO 10, and PESO 15 showed a new linear region that we called Linear 1, associated with the mechanical contribution of the coating, and replaced the toe and heel regions. In Table 2, the modulus of the Linear 1 and Linear 2 (referring to the linear region previously cited) regions are reported for the different samples. As can be noticed, the moduli of Linear 1 were the same without any significant difference (ANOVA test, $p < 0.05$), confirming that the Linear 1 region was determined by the coating on the substrate. Similarly, the ANOVA test did not show any significant difference between the moduli of Linear 2, the region associated with FL. The mechanical properties of the coating had a visible impact on the FL, hiding the contribution of the substrate in terms of toe and heel regions, confirming that the coating was not an on-top layer but stably linked to the fibrillary structure of the FL. However, the presence of the Linear 2 region confirmed that the FL maintained its flexibility even in the presence of the coating. This result was really appreciated because the FL maintained its workability and softness, two of the main advantages of the FL over cow leather. This result

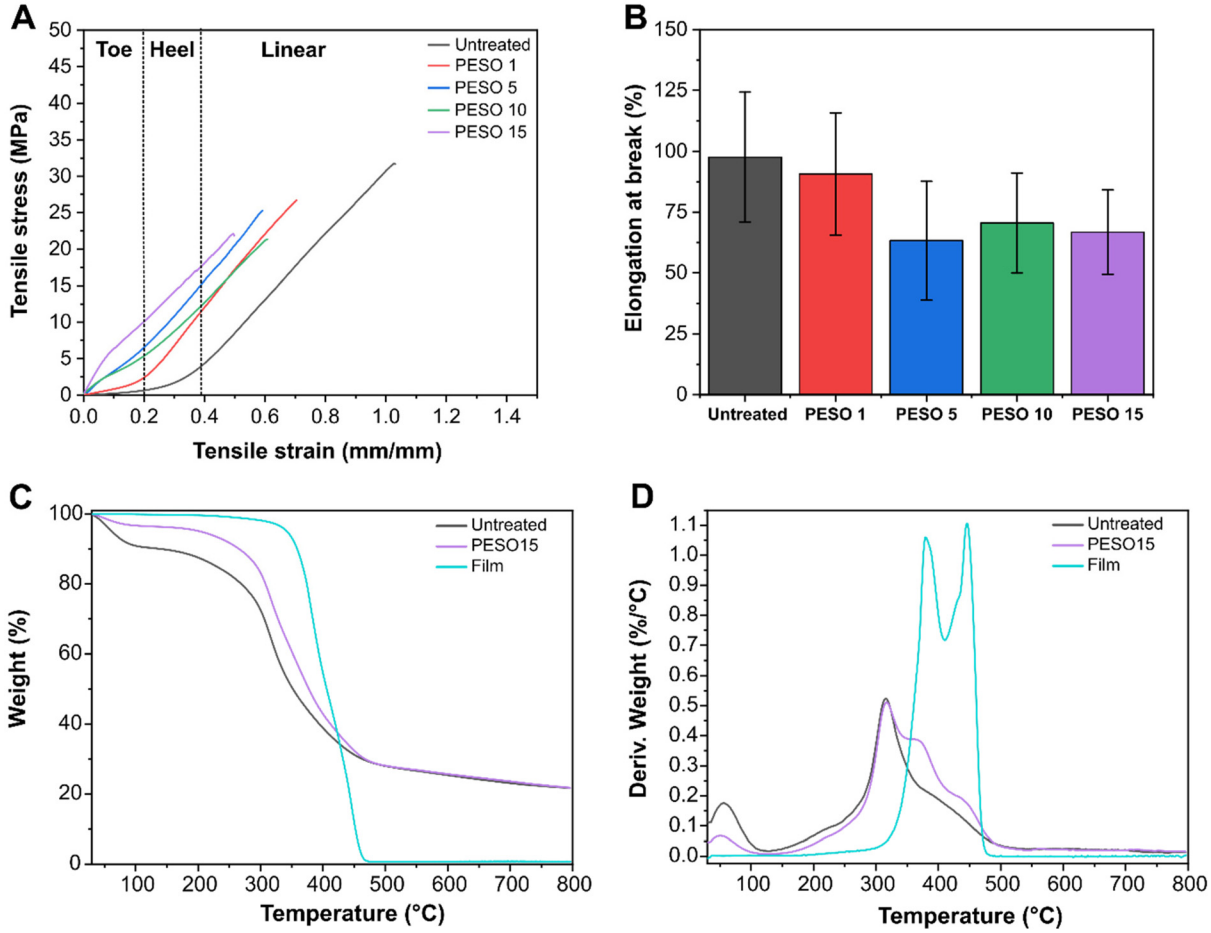

Fig. 6 (A) Stress–strain curves of untreated FL, PESO 1, PESO 5, PESO 10, and PESO 15. (B) Elongation at break (%) of untreated FL, PESO 1, PESO 5, PESO 10, and PESO 15. The ANOVA test was performed for $p < 0.05$. (C) Mass loss and (D) derivatives of the thermograms of untreated FL, PESO 15 and film.

Table 2 Modulus (MPa) of the two linear regions individuated by the stress–strain curves of the untreated FL, PESO 1, PESO 5, PESO 10 and PESO 15. *ANOVA test ($p < 0.05$)

Sample	Linear 1 – modulus ± s.d. (MPa)*	Linear 2 – modulus ± s.d. (MPa)*
Untreated	—	38.99 ± 16.93
PESO 1	—	45.97 ± 18.83
PESO 5	55.12 ± 19.45	61.36 ± 15.13
PESO 10	51.38 ± 30.06	45.89 ± 21.90
PESO 15	55.94 ± 20.08	41.99 ± 13.31

was also confirmed by the evaluation of ductility in terms of elongation at break (Fig. 6B). The ANOVA test ($p < 0.05$) did not reveal any significant difference between the samples confirming that the coating, in the quantity deposited, did not change the ductility of the FL but it was determined solely by the substrate.

3.8. Thermal characterization

The thermal stability of PESO 15 was evaluated and compared with two controls, untreated FL and film sample, by TGA. The thermograms and the derivatives of weight loss curves are reported in Fig. 6C and D. As can be noticed, untreated FL presented a two steps weight loss. The first peak was at 56 °C and presented a 10% weight loss due to the loss of structural water bonds, while the second one was at 315 °C and presented a 60% weight loss due to the thermal destruction of the polypeptide chain.[34] On the other hand, PESO 15 coated fish leather presented four thermal peaks. The first two peaks were at the same temperature as untreated FL, whereas the only difference was in the 3% weight loss after the first peak compared to the 10% observed for the untreated FL. This fact might be explained by the fact that PESO coating reduced moisture absorption protecting the FL from thermal degradation at this early stage and, therefore, improving its thermal stability. The other two peaks at 379 °C and 445 °C were associated with the degradation of the coating as confirmed by the derivative thermogram of the free standing film, as previously observed for ESO.[15]

3.9. Application of the coating on cotton

Cotton is the main natural fiber used for textile applications. Cotton textile is made of cellulose fibers weaved into fabrics.

Being made of cellulose, cotton has a similar strong interaction with water, which is readily absorbed in the material. While the surface chemistry of FL showed carboxyl, amino and hydroxyl groups, the surface chemistry of cotton is dominated by hydroxyl groups. To test the ability of the coating to protect cotton, and, from the perspective of other cellulose-based materials, PESO 15 coating was applied on cotton textile. The same steps to apply and cure the coating developed for FL were applied on cotton.

The microstructure of the untreated and treated cotton samples was analyzed by SEM and results are shown in Fig. 7. As can be noticed in the inset pictures, the coating changed the color of the cotton from white to yellowish. In spite of this, no differences in the microstructure of the cotton were visible. The cross section at low magnification did not show visible differences, because the coating, as shown in the higher magnification in Fig. 7D, is very thin (<100 nm) and conformal to the single fiber. Therefore it did not alter the microstructure of the inter-weaved fibers. Since the complex structure of the collagen fibers in FL did not allow us to have clear and precise imaging, we hypothesize that a microstructure similar to the one seen for cotton was obtained.

The hydrophobicity of the coated cotton was evaluated by measuring the WCA and WVP. As expected, untreated cotton revealed a hydrophilic behavior, while, as can be seen from Fig. 7E, PESO15 coated cotton, showed a significant hydrophobic character with a WCA of around 148°, a value that is very close to the 150° limit conventionally associated with superhydrophobicity. Using the model of eqn (6), σ_c for the cotton was found to be 0.20, a value lower than that of fish leather, probably due to the lower density of fibers on the cotton's surface. Looking at the change of WCA with time, this

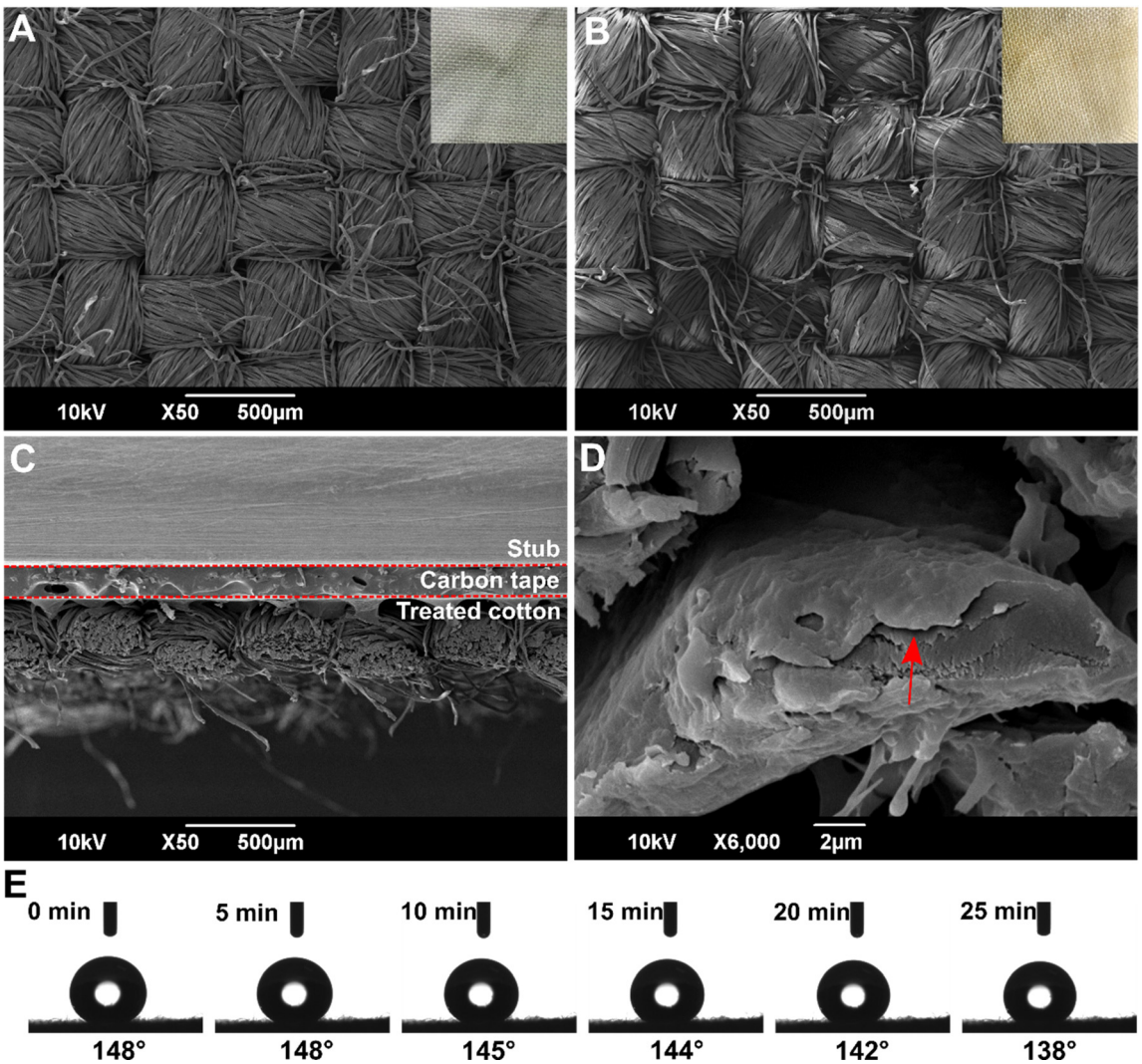

Fig. 7 (A) SEM image of the surface of untreated cotton. Photo of the sample is reported in the top-right corner. (B) SEM image of the surface of treated cotton. Photo of the sample is reported in the top-right corner. (C) SEM image of the cross section of the treated cotton. (D) SEM image of the cross section of the treated cotton with ×6000 magnification. The red arrows highlight the coating on the cotton fiber. (E) Photos of the water drop (10 μL) on treated cotton with the value of the respective contact angle every 5 minutes for 25 minutes.

hydrophobic character was preserved for the first 25 min, with WCA only slightly decreasing to 138°, while the drop base diameter did not change. As discussed before, this behavior is associated with water evaporation. At 30 min, the WCA decreased at 90° and at 35 min it decreased below 90°. In addition, the volume drastically decreased while the drop base diameter increased: water was absorbed by the sample. Therefore, in conclusion, after 25 minutes the water resistance property of the coating on cotton was lost, compared to the 40 minutes of the treated fish leather. The most probable explanation for this difference between cotton and FL is based on the surface chemistry of cotton. As previously demonstrated by Mazzon *et al.*,[35] the functional groups on the surface of cotton are due to the cellulose fibers that show mainly –OH groups, without the carboxylic groups and amines of collagen. The reactivity of –OH groups with the epoxide ring is lower than carboxyl and amino groups, therefore, during curing, ESO binds preferentially with the carboxylic groups of Pripol and a weaker bond with the –OH groups of the cotton is formed.

In addition, the WVP of the untreated and treated cotton was evaluated by using the previously described method to understand if the coating affected the breathability of cotton. The WVP, resulted in $(1.95 \pm 0.09) \times 10^{-4}$ g (m day Pa)$^{-1}$ and $(2.08 \pm 0.07) \times 10^{-4}$ g (m^2 day Pa)$^{-1}$, for the untreated and treated cotton, respectively, without any significant difference between them (ANOVA, $p < 0.05$), therefore the coating did not affect the breathability of cotton. A similar behavior on cotton was previously observed by Mazzon *et al.*, demonstrating that the presence of a polyurethane coating did not change the permeability of the cotton substrate.[35]

4. Conclusion

In this work, two by-products of the food industry, epoxidized soybean oil (ESO) and fatty acid derived Pripol, were considered as fully sustainable alternatives to fluorine chemistry and the use of nanoparticles to impart hydrophobicity to a discarded biomass of the food industry, salmon fish skin, which was valorized as fish leather (FL), with the final aim of fulfilling the requirements of the fashion industry: protecting FL from water and moisture. Pripol and ESO were combined to obtain a crosslinked material and were applied as a coating to improve the wettability properties of the FL. The coating was deposited by simple dip coating and the crosslinking could be performed at the low temperatures required by the FL, creating a strong network with a high gel fraction. The fast water absorption of FL, individuated as the main drawback in its application, was overcome thanks to the oil-based coating, even if its combination with FL not only imparted hydrophobicity with WCAs comparable to PTFE, but also maintained this property during time as demonstrated by monitoring the WCA. In particular, the PESO 15 coating was demonstrated to be the most effective in terms of hydrophobicity and durability of this property. In addition, the coating had a protective effect against humidity in particular at realistic R.H. %, between 44 and 84%, decreasing the water uptake of the FL from 17 to 12%. The PESO can be deposited as a thin and conformable coating, providing water protection without affecting the FL's microstructure, and, therefore, its breathability, ductility and softness, all appealing properties of FL compared to the more used cow leather. In addition, the coated FL maintained its hydrophobicity after soaking in water, showing stable water protection. Finally, the functionality of the coating was assessed on an alternative textile substrate, such as cotton, broadening the possibility of application.

Conflicts of interest

There are no conflicts to declare.

Acknowledgements

The authors would like to acknowledge the H2020 RISE FISHSKIN Project, Grant Agreement No. FISHSkin 823943 and ViaTalenta Foundation for providing the salmon leather, and would like to thank Dr Lara Marini for TGA measurements and Milad Safarpour (Smart Materials, IIT) for helping with curing PESO with a catalyst, the Materials Characterization Facility (IIT) and the Electron Microscopy Facility (IIT).

References

1 L. Frühe, T. Cordier, V. Dully, H. W. Breiner, G. Lentendu, J. Pawlowski, *et al.*, Supervised machine learning is superior to indicator value inference in monitoring the environmental impacts of salmon aquaculture using eDNA metabarcodes, *Mol. Ecol.*, 2021, **30**(13), 2988–3006.
2 L. Burridge, J. S. Weis, F. Cabello, J. Pizarro and K. Bostick, Chemical use in salmon aquaculture: a review of current practices and possible environmental effects, *Aquaculture*, 2010, **306**(1–4), 7–23.
3 G. L. Taranger, Ø. Karlsen, R. J. Bannister, K. A. Glover, V. Husa, E. Karlsbakk, *et al.*, Risk assessment of the environmental impact of Norwegian Atlantic salmon farming, *ICES J. Mar. Sci.*, 2015, **72**(3), 997–1021.
4 E. Palomino, G. Defeo and others, *Material Design Innovation: Fish Leather, a new environmentally friendly material*, 2018.
5 V. R. Sherman, W. Yang and M. A. Meyers, The materials science of collagen, *J. Mech. Behav. Biomed. Mater.*, 2015, **52**, 22–50.
6 J. Ma, X. Zhang, Y. Bao and J. Liu, A facile spraying method for fabricating superhydrophobic leather coating, *Colloids Surf., A*, 2015, **472**, 21–25.
7 O. Serenko, Z. Nizamova, M. Kalinin, Y. Ostrovsky, L. Polukhina and A. Muzafarov, Effect of the morphology of leather surface on the hydrophobic-hydrophilic properties, *Adv. Mater. Phys. Chem.*, 2014, **2014**(4), 13–19.

8 M. Boström and M. Micheletti, Introducing the sustainability challenge of textiles and clothing, *J. Consum. Policy*, 2016, **39**, 367–375.
9 T. T. Qiang, X. Luo, L. F. Ren, X. C. Wang and B. Y. He, Preparation, characterization of silicone succinate ester and its application in leather industry, *Adv. Mater. Res.*, 2011, **197**, 409–416.
10 F. Ye, X. Liao, Y. Wang and B. Shi, Improvements in Leather Surface Hydrophobicity through Low-pressure Cold Plasma Polymerization, *J. Am. Leather Chem. Assoc.*, 2014, **109**(03), 89–95.
11 V. Kadam, S. K. Chattopadhyay, A. Raja and D. Shakyawar, Waste management in coated and laminated textiles, *Waste Manag. Fash Text Ind.*, 2021, 215–231.
12 S. Joshi, P. R. Gogate, P. F. Moreira Jr. and R. Giudici, Intensification of biodiesel production from soybean oil and waste cooking oil in the presence of heterogeneous catalyst using high speed homogenizer, *Ultrason. Sonochem.*, 2017, **39**, 645–653.
13 K. Saremi, T. Tabarsa, A. Shakeri and A. Babanalbandi, Epoxidation of soybean oil, *Ann. Biol. Res.*, 2012, **3**(9), 4254–4258.
14 X. Ge, L. Yu, Z. Liu, H. Liu, Y. Chen and L. Chen, Developing acrylated epoxidized soybean oil coating for improving moisture sensitivity and permeability of starch-based film, *Int. J. Biol. Macromol.*, 2019, **125**, 370–375.
15 S. Miao, K. Liu, P. Wang, Z. Su and S. Zhang, Preparation and characterization of epoxidized soybean oil-based paper composite as potential water-resistant materials, *J. Appl. Polym. Sci.*, 2015, **132**(10), 41575.
16 A. Demongeot, S. Mougnier, S. Okada, C. Soulié-Ziakovic and F. Tournilhac, Coordination and catalysis of Zn2+ in epoxy-based vitrimers, *Polym. Chem.*, 2016, **7**(27), 4486–4493.
17 W. J. Blank, Z. He and M. Picci, Catalysis of the epoxy-carboxyl reaction, *J. Coat. Technol.*, 2002, **74**, 33–41.
18 S. Liang, K. Xu, H. Liu, X. Gui and T. Zhang, Preparation and characterization of dimer fatty acid epoxy-acrylate resin hybrid emulsion for photocurable coatings, *Colloid Polym. Sci.*, 2019, **297**, 1199–1211.
19 Y. Li, T. Liu, S. Zhang, L. Shao, M. Fei, H. Yu, *et al.*, Catalyst-free vitrimer elastomers based on a dimer acid: robust mechanical performance, adaptability and hydrothermal recyclability, *Green Chem.*, 2020, **22**(3), 870–881.
20 S. J. Park, F. L. Jin and J. R. Lee, Thermal and mechanical properties of tetrafunctional epoxy resin toughened with epoxidized soybean oil, *Mater. Sci. Eng., A*, 2004, **374**(1–2), 109–114.
21 H. Barcena, A. Tuachi and Y. Zhang, Teaching green chemistry with epoxidized soybean oil, *J. Chem. Educ.*, 2017, **94**(9), 1314–1318.
22 A. Adhvaryu and S. Erhan, Epoxidized soybean oil as a potential source of high-temperature lubricants, *Ind. Crops Prod.*, 2002, **15**(3), 247–254.
23 Z. S. S. Júnior, S. B. Botta, P. A. Ana, C. M. França, K. P. S. Fernandes, R. A. Mesquita-Ferrari, *et al.* Effect of papain-based gel on type I collagen-spectroscopy applied for microstructural analysis, *Sci. Rep.*, 2015, **5**(1), 11448.
24 H. Xiao, G. Cai and M. Liu, Hydroxyl radical induced structural changes of collagen, *Spectroscopy*, 2007, **21**(2), 91–103.
25 K. W. Sanden, A. Kohler, N. K. Afseth, U. Böcker, S. B. Rønning, K. H. Liland, *et al.*, The use of Fourier-transform infrared spectroscopy to characterize connective tissue components in skeletal muscle of Atlantic cod (Gadus morhua L.), *J. Biophotonics*, 2019, **12**(9), e201800436.
26 P. M. Wairimu, E. W. Nthiga and M. A. Ollengo, *The structural and chemical properties of the nile perch fish leather*, 2020.
27 R. Nogami, N. Kaku, T. Shimada, T. Tabata, H. Tagomori and H. Tsumura, Three-dimensional architecture of the acetabular labrum in the human hip joint, *Med. Mol. Morphol.*, 2020, **53**, 21–27.
28 J. Zhang, Q. Shang, Y. Hu, G. Zhu, J. Huang, X. Yu, *et al.*, Castor-oil-based UV-curable hybrid coatings with self-healing, recyclability, removability, and hydrophobicity, *Prog. Org. Coat.*, 2022, **165**, 106742.
29 P. Parvathy and S. K. Sahoo, Hydrophobic, moisture resistant and biorenewable paper coating derived from castor oil based epoxy methyl ricinoleate with repulpable potential, *Prog. Org. Coat.*, 2021, **158**, 106347.
30 S. P. Vijayan, S. Aparna and S. K. Sahoo, Effect of beeswax on hydrophobicity, moisture resistance and transparency of UV curable linseed oil based coating for compostable paper packaging, *Ind. Crops Prod.*, 2023, **197**, 116645.
31 E. Bormashenko, Y. Bormashenko, T. Stein, G. Whyman and E. Bormashenko, Why do pigeon feathers repel water? Hydrophobicity of pennae, Cassie–Baxter wetting hypothesis and Cassie–Wenzel capillarity-induced wetting transition, *J. Colloid Interface Sci.*, 2007, **311**(1), 212–216.
32 Y. Xiang, P. Fulmek, D. Platz and U. Schmid, Temperature dependence of water contact angle on teflon AF1600, *Langmuir*, 2022, **38**(4), 1631–1637.
33 T. Gutsmann, G. E. Fantner, J. H. Kindt, M. Venturoni, S. Danielsen and P. K. Hansma, Force spectroscopy of collagen fibers to investigate their mechanical properties and structural organization, *Biophys. J.*, 2004, **86**(5), 3186–3193.
34 G. Ramanathan, S. Singaravelu, M. Raja, S. Sobhana and U. T. Sivagnanam, Extraction and characterization of collagen from the skin of Arothron stellatus fish—A novel source of collagen for tissue engineering, *J. Biomater. Tissue Eng.*, 2014, **4**(3), 203–209.
35 G. Mazzon, M. Zahid, J. A. Heredia-Guerrero, E. Balliana, E. Zendri, A. Athanassiou, *et al.*, Hydrophobic treatment of woven cotton fabrics with polyurethane modified aminosilicone emulsions, *Appl. Surf. Sci.*, 2019, **490**, 331–342.